

Vascularization Of The Hippocampus

Oluwatobi Folorunsho Adeyemi

University Of Abuja, Department Of Physics, Abuja

Abstract

This initial study aimed at identifying the potential of non-contrast imaging methods to map the vasculature of the hippocampus in vivo and give detail understanding of its role in neurodegenerative diseases.

We use high-resolution time-of-flight (TOF) image, to successfully identified major hippocampal arteries, including the posterior cerebral artery (PCA) and anterior choroidal artery (AChA), and classified hippocampal arterial networks into distinct groups based on established anatomical classifications. Also, Susceptibility-Weighted Imaging (SWI) was used to visualised of small veins around the hippocampus, which usually required contrast agents or cadaver studies.

Our findings show the potential of these non-invasive imaging techniques to provide detailed views of hippocampal vasculature, showing a consistent pattern of arteries and veins that align with previous cadaveric studies. By mapping of these vascular networks, this study sets the stage for future investigations into the relationship between hippocampal vascular changes and degenerative pathology, particularly in neurodegenerative diseases such as Alzheimer's disease (AD).

The ability to detect variations in arterial and venous diameters may provide new insights into the triggers and progression of neurodegenerative conditions, showing the importance of advanced imaging modalities in clinical research and practice.

Keyword: *Hippocampus, 7T MRI, Artery and Vein*

Date of Submission: 20-08-2024

Date of Acceptance: 30-08-2024

I. Introduction

The hippocampus is a highly complex and important brain structure that is involved in various cognitive functions, including memory consolidation, spatial navigation, and pattern separation (Manjon et al., 2020). Its degeneration is a hallmark of Alzheimer's disease (AD) and is often used as a diagnostic criterion for this disease (Braak & Braak, 1991). The measurement of hippocampal volume using magnetic resonance imaging (MRI) has become a valuable tool for the follow-up and treatment adjustment of AD patients (Jack et al., 2005). The hippocampus is divided into subfields, such as the dentate gyrus and Cornu Ammonis (CA) regions, which can be segmented and measured using automated segmentation techniques like Automatic Segmentation of Hippocampal Subfields (ASHS) (Yushkevich et al., 2015)

However, it is challenging to obtain in vivo studies of the vasculature of the hippocampus due to its location deep within the brain. Nonetheless, non-invasive in vivo studies are crucial for both healthy and diseased participants, providing valuable information for both neuroscience and neurology applications. Most investigations of the hippocampus are usually based on histology or post-mortem studies, which provide limited information about its dynamic function. Therefore, non-invasive in vivo studies are essential to better characterise the anatomy and ultimately to investigate the links between anatomy and function, particularly in understanding the mechanisms underlying neurodegenerative diseases like Alzheimer's.

The posterior cerebral artery (PCA) provides the primary supply to the anterior choroidal artery (AChA) (Spallazzi et al., 2019). These two arteries are the main vessels that supply blood to the hippocampus, individually or mixed. The hippocampal head is supplied by the anterior hippocampal artery (AH) and the uncus, while the hippocampal body and tail are supplied by the middle and posterior hippocampal arteries (MH and PH), respectively. The naming of the arteries is related to the part they supply (Marinković et al., 1992, Prades et al., 1993). However, considering the vasculature in more detail, a recent study by (Isolan et al., 2020) classified the hippocampal arterial vasculature of individuals into six groups, as shown in Figure 1:

- Group A: This group presents mixed irrigation, with the hippocampal arteries originating from the anterior choroidal, PCA, anterior infratemporal artery (AIA), and splenic artery (SA).
 - Group B: The hippocampal arteries originate from the temporal branches, such as the main inferotemporal trunk, middle inferotemporal artery (MITA), posterior inferotemporal artery, or the main branch of PCA.
 - Group B2: In this case, the inferior temporal arteries arise from a common trunk, with an arrowhead identifying a common inferior temporal artery.
-

- Group C: The anterior inferior temporal artery (AITI) is the main feeder of the hippocampus.
- Group D: The hippocampal arteries originate from the posterior cerebral artery's (PCA) main trunk, and they are the largest contributors to the hippocampus blood supply in this group.
- Group E: A single trunk of the posterior cerebral artery (named Ushimura's artery), with its origin at the main branch of PCA, irrigates practically the entire hippocampus.
- Group F: The hippocampal vessels arise exclusively from the parieto-occipital artery (POA), calcarine artery (CA), and the SA.

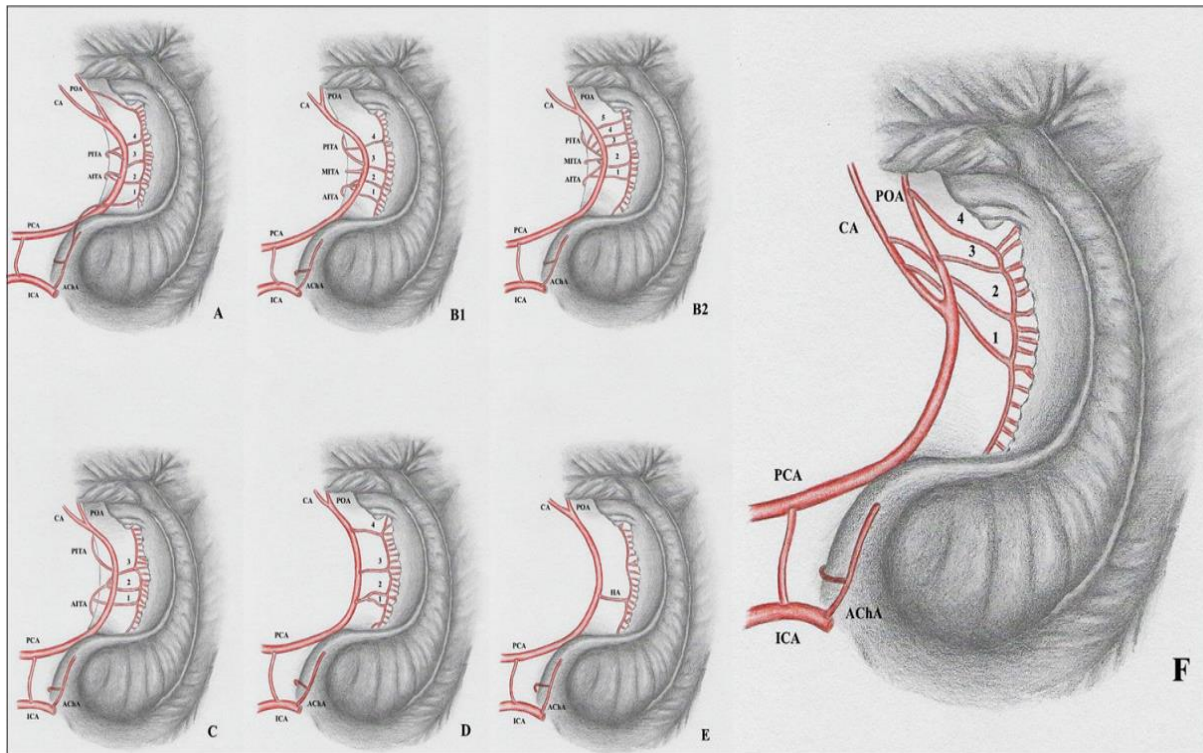


Figure 1: pictorial representation of different group categorizations of hippocampal arterial supply, showing the intra and extraventricular view of the hippocampus. See text for further explanation. CA: Calcarine artery; ICA: Internal carotid artery, PCA: Posterior cerebral artery, POA: Parieto-occipital artery, AITA: Anterior inferior temporal artery, MITA: Medial inferior temporal artery, PITA: Posterior inferior temporal artery, AChA: Anterior choroidal artery. 1, 2, 3, and 4: Hippocampal arteries'. (Isolan et al., 2020).

The hippocampus venous drainage has received less attention due to the technical challenges involved in studying it. However, the branches of the basal vein are known to be the main veins that drain blood from the hippocampus (Henri Duvernoy, Françoise Cattin, 2013). Within the hippocampus, two main veins can be distinguished: the sulcal intrahippocampus vein and the subependymal intrahippocampus veins (Henri Duvernoy, Françoise Cattin, 2013). The sulcal intrahippocampus vein is located between the Cornu Ammonis and the gyrus dentatus, while the subependymal intrahippocampus veins drain blood from the deep layers of the CA2, CA1 and subiculum. Knowledge of the hippocampal venous drainage is important for understanding the role of the hippocampus in cerebral blood flow regulation and in the pathophysiology of various diseases. For instance, venous congestion may lead to hypoxia and ischemia, which could damage the neurons in the hippocampus and cause cognitive impairment (Fulop et al., 2019). Therefore, further studies are needed to better understand the venous drainage of the hippocampus and its clinical implications.

Studying the vasculature of the hippocampus in detail has been challenging in the past due to the small size of the arteries and veins, ranging between 0.2 and 1.0 mm in diameter. Most of the studies involving the vasculature of the hippocampus have been carried out using cadavers. However, with the advent of higher static field scanners (7T and above), we can use high-resolution angiography and venography to study the small vessels in vivo (Spallazzi et al., 2019).

In this study, we utilized high-resolution TOF-MRA images to identify the arteries around the hippocampus, while a single-echo T₂*-weighted 3D GRE sequence was used to generate the susceptibility-weighted imaging (SWI) to identify the venous supply of the hippocampus.

II. Methods

The study was conducted at the Sir Peter Mansfield Imaging Centre at the University of Nottingham in the UK. Image acquisition was carried out using a whole-body Philips ACHIEVA 7 T system, equipped with a Nova Medical (Wilmington MA, USA) single-channel transmit, and 32-channel receive (1Tx32Rx) head coil.

For the venography a T_2^* single echo image was acquired perpendicularly to the long axis of the hippocampus to highlight the very tiny venous structure and was processed into a SWI. The scan had the following parameters; $0.38 \times 0.37 \times 0.74 \text{ mm}$ reconstructed at $0.35 \times 0.35 \times 0.37 \text{ mm}$ TR = 24 ms, TE = 18 ms, FA = 8° , Water-fat shift was set at 7 pixels and bandwidth at 144.6 Hz, and a practical optimization of the trade-off between SNR and distortion in the SWI; the acquisition time was 06:39 min.

The last set of images acquired was TOF angiography. We optimized this scan to maximise saturation of tissue and minimise saturation of inflow blood, in the shortest possible time, covering the entire hippocampus and at a resolution of 0.38 mm isotropic using 4 packages, TR = 14 ms, TE = 4.5, FA = 22° the TA was 06:07 min.

To locate the hippocampus for later scans and for hippocampal segmentation, a T_1 -weighted PSIR image was acquired with the following parameters: 0.55 mm isotropic resolution, TR = 6.9 ms, TE = 5.1 ms, 348 number of slices and an acquisition time of 12:25 minutes.

To assist with segmenting the hippocampus a T_2 -weighted FSE scan was also acquired with voxel size of $0.375 \times 0.375 \times 1.5 \text{ mm}$, TR = 5500ms, TE = 119 ms and an acquisition time of 04:24 minutes.

All participants included in the study provided informed written consent, as approved by the protocol ethics.

Hippocampal Segmentation

The hippocampus segmentation was performed using Automatic Segmentation of Hippocampus Subfield (ASHS), a software developed by (Yushkevich et al., 2015). Fig 2 shows a 3D representation of the segmentation obtained from ASHS and the segmentation overlaid on a T_2 -weighted image. To ensure the accuracy of the segmentation, the segmented hippocampus mask was inspected using both FSLEyes and MeVisLab (MeVis, Bremen, Germany). MeVisLab is a powerful framework for image processing of 2D and 3D medical imaging data sets and offers rapid prototyping, a wide range of features, supported file formats, and extensibility options.

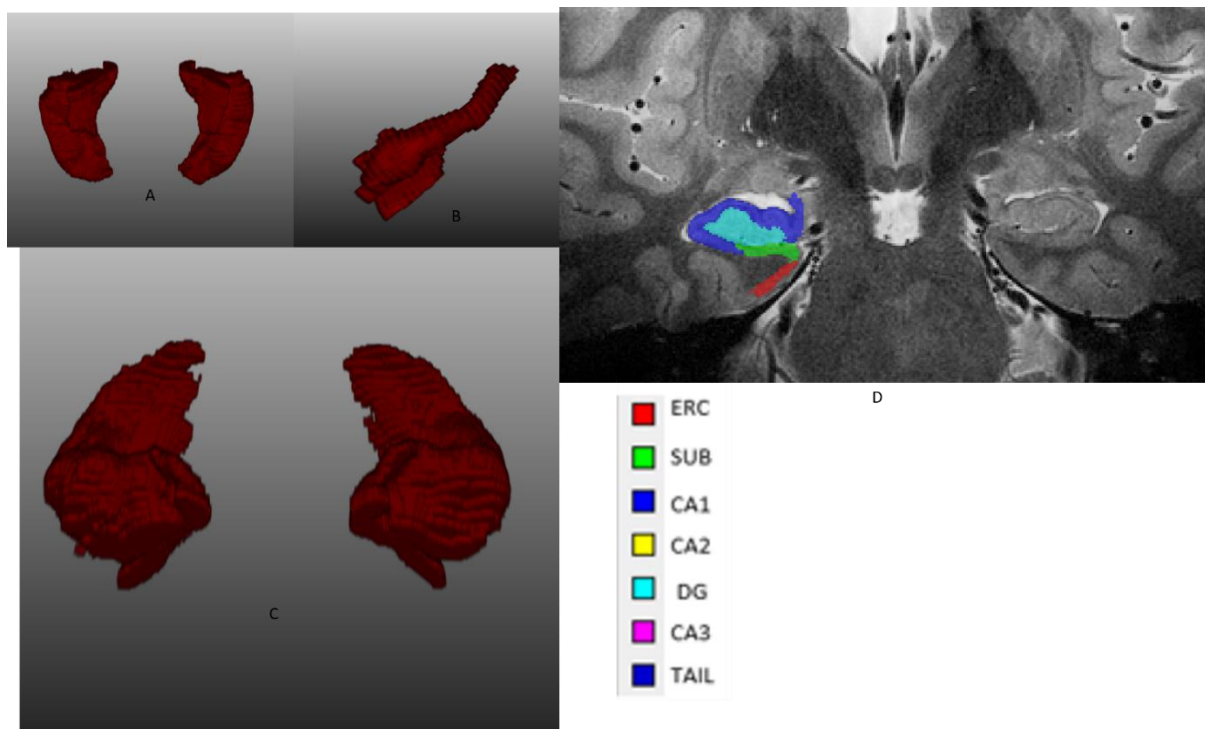


Figure 2: The Axial, sagittal and coronal view of the hippocampus segmentation and it overlaid on the T_2 -weighthed.

Tof Angiography Data

The TOF images shown in the figure below were obtained for each participant in this study and were used for identifying the arteries around the hippocampus.

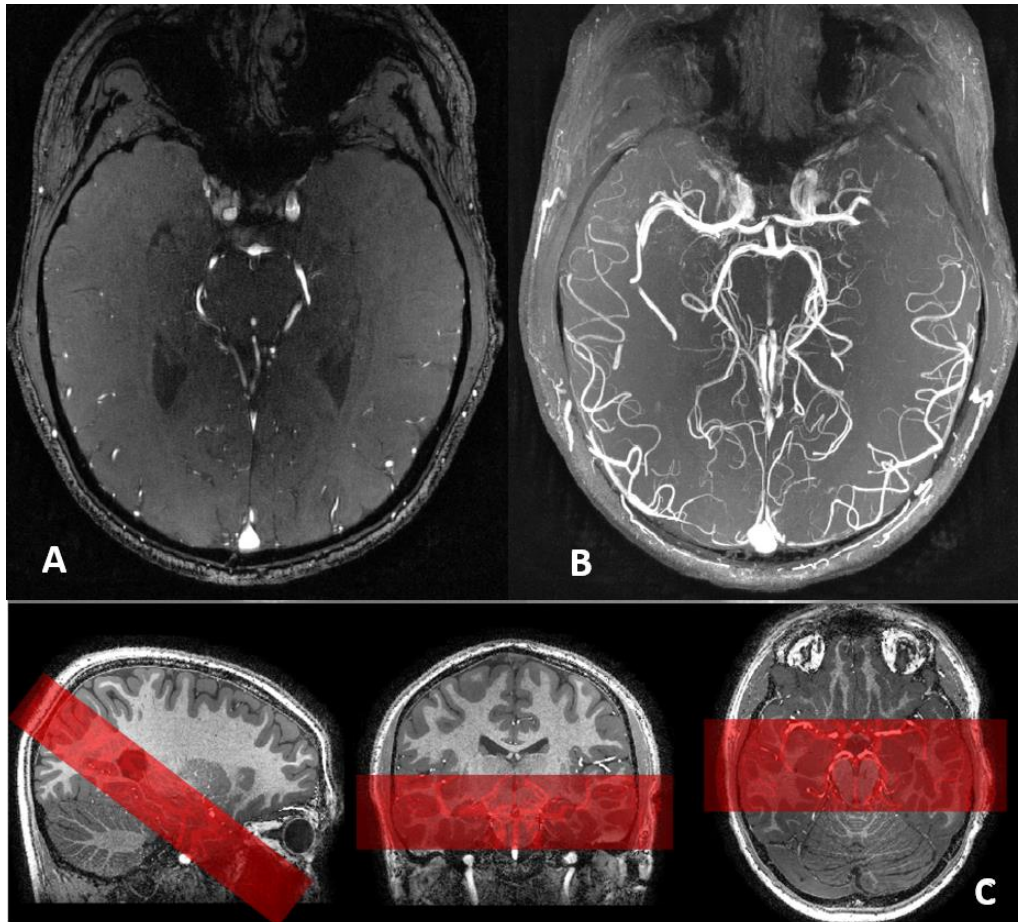


Figure 3: A) The Time of Flight (TOF) B) the maximum intensity projection of the TOF for one of the participants in the study and C) the TOF (red) covering the entire hippocampus as acquired from the scanner.

To be able to visualise the tiny arteries around the hippocampus, TOF images were acquired covering the entire hippocampus as quickly as possible, to generate good contrast at a high resolution, as shown in Fig 3.

TOF-MRA were registered to the hippocampus mask, using FLIRT on FSL (Jenkinson et al., 2002), to avoid misidentification of the hippocampus artery (this helped eliminated arteries that were not connected to the hippocampus).

The TOF data was visualised using Maximum Intensity Projection software available in MeVisLab to identify the arteries, especially the posterior cerebral artery (PCA) and the anterior choroidal artery (AChA) as shown in Fig 5. The registered image was thresholded to extract just the signal from the arteries, with every pixel with signal below the threshold made zero. A single threshold for each data set was selected manually, depending on the intensity of the image. The thresholding the TOF needed to be selected very carefully as it tended to lead to loss of smaller vessels.

SWI Data

The SWI data were generated using the method described by (Haacke et al., 2004). Firstly, the phase image from the GRE data set is passed through a complex high pass filter to remove any artefacts and slowly varying phase shifts. The phase mask generated through this process is then multiplied by the magnitude image five times in MATLAB (R2020b, Mathworks, Inc., Natick, MA USA). This combination enhances the T_2^* contrast with phase information and enables the identification of the venous supply of the hippocampus with high sensitivity. In the SWI images the paramagnetic deoxyhaemoglobin in the venous blood causes a signal dropout in the veins, making them appear dark in the SWI (compared to the original magnitude image as shown in Figure 4).

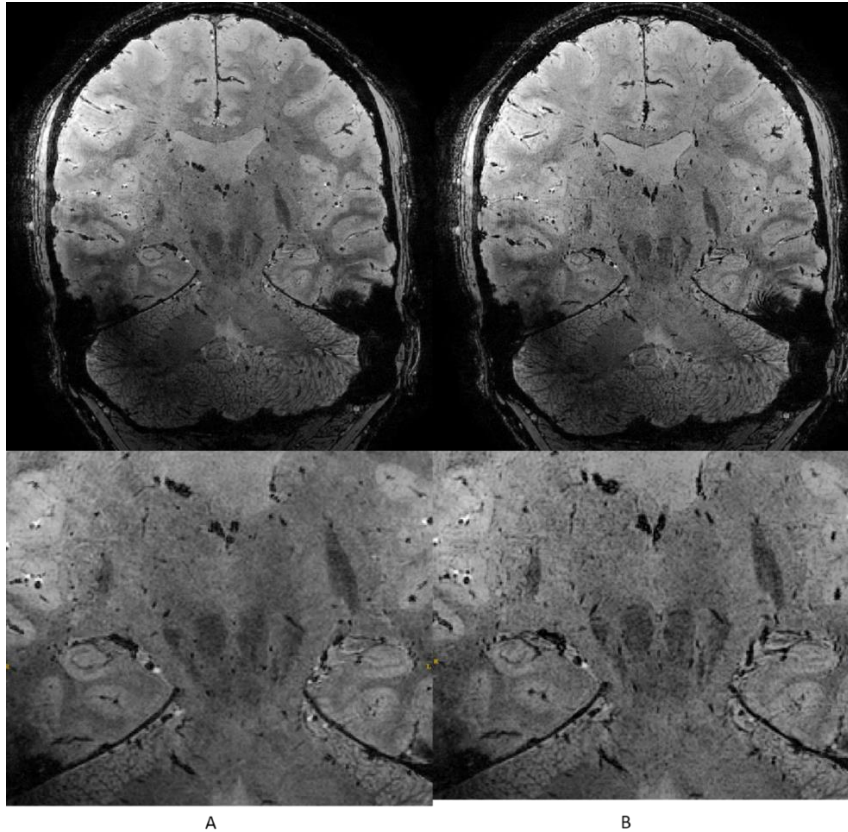


Figure 4: shows A) the magnitude image of the SE T₂* sequence and B) the magnitude image of the SWI obtained after processing A.

After obtaining the SWI image, it was processed using MATLAB to segment the hippocampal veins. MeVisLab could not be simply used because of the reverse contrast of the SWI images. Firstly, the SWI was manually thresholded to identify the lowest signal potentially corresponding to the veins. This method has limitations as low signals from iron-rich tissues such as the Red Nucleus may lead to a loss of signal of smaller vessels, so a mask was used to remove such areas. Signals less than the threshold were set to zero, and signals greater than or equal to the threshold were set to one. The resulting vessel mask was then inverted, making the veins the brightest signals in the image, using ‘imcomplement’ function on MATLAB. The image was then denoised by removing voxels with less than 50 voxels connected to them, this was done by using the ‘bwareaopen’ function in MATLAB, which remove all connected component that contain fewer than 50 voxels in the T₂* image, as those are considered to be noise. To identify the veins around the hippocampus, the denoised image was multiplied by a dilated mask of the hippocampus to avoid overlap from surrounding veins in the maximum intensity projections (MIPs). The resulting 3D image of the veins was finally visualized using MeVisLab software, as shown in Fig 5.

III. Results

Here we present the results of the eight participants involved in this study. The subject demographics are given in Table 1. The groups to which the arteries were considered to fall are also given in Table 1.

	Age	Sex	Group
Subject 1	31	Female	Group A
Subject 2	23	Male	Group E
Subject 3	25	Male	Group C
Subject 4	28	Female	Group D
Subject 5	31	Male	Group F
Subject 6	59	Female	Group F
Subject 7	33	Female	Group F
Subject 8	20	Male	Group F

Table 1: Subject demographics and assigned group for arteries.

A consistent pattern emerges from these visual representations, showing the consistent arrangement of veins and arteries around the hippocampal region. Nonetheless, individual anatomical distinctions contribute to some variations within this pattern.

A noteworthy comparison can be drawn between our findings and the schematic representation of vascularization patterns as categorized by (Isolan et al., 2020). Notably, Isolan et al.'s classification encompasses six distinct patterns, thereby offering an additional layer of insight into the hippocampal vasculature.

Figure 5 provides a comparative analysis between our findings and those presented in a cadaver study by (Wen et al., 1999). Through this comparison, we match certain arteries and veins obtained from subj07 with the corresponding anatomical structures depicted in the inked cadaver image. This parallel assessment shows the alignment of our *in vivo* imaging outcomes with the anatomical information derived from a cadaveric context.

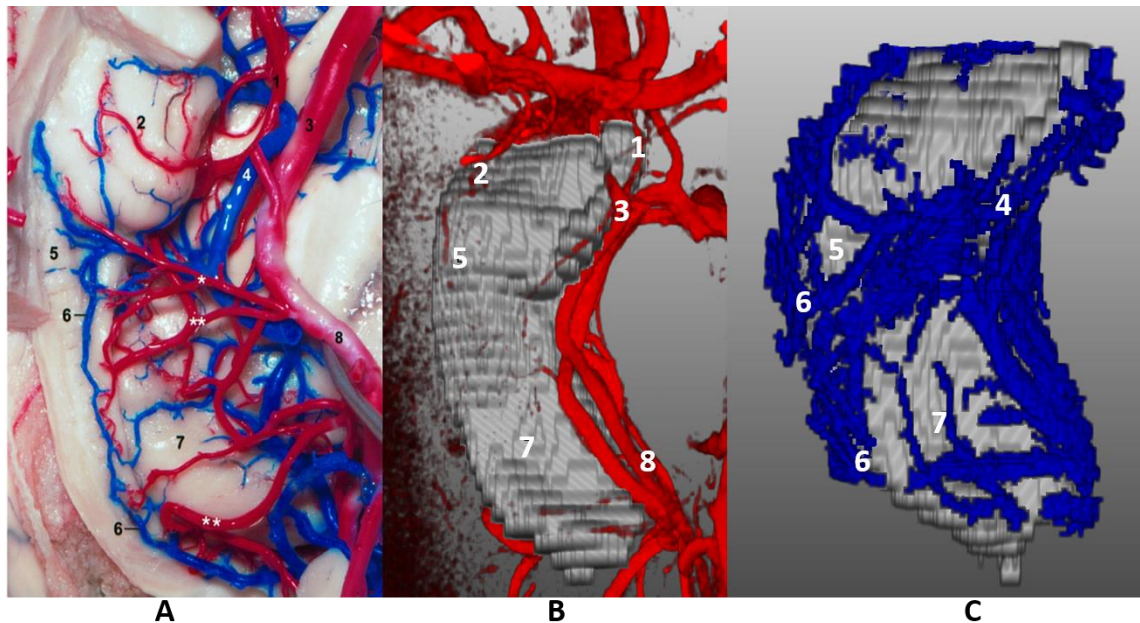


Figure 5: comparing A) the Cadaver image of the hippocampus (Wen et al., 1999) with B) our image of the arteries overlaid on the hippocampus and C) veins overlaid on the hippocampus. 1, anterior choroidal artery; 2, inferior surface of the posterior segment of the uncus; 3, P2A segment of the posterior cerebral artery; 4, basal vein; 5, dentate gyrus and fimbria; 6, anterior and posterior longitudinal hippocampal veins; 7, pulvinar of the thalamus; 8, P2P segment of the posterior cerebral artery; *, hippocampal arteries; **, lateral posterior choroidal artery.

IV. Discussion

In this preliminary investigation, we have explored the potential of non-contrast imaging methods to map out the intricate vasculature of the hippocampus *in vivo*. By doing so, we identified the major arteries and veins responsible for supplying and draining blood from the hippocampus in individual subjects. This preliminary insight holds promise for further investigations into the relationship between hippocampal vasculature and degenerative pathology. In a study of an AD model in mice, a reduction in diameter of the artery that supply blood to the hippocampus (Dentate Gyrus) was observed together with a change in the vasculature pattern (Zhang et al., 2019).

To delineate the arterial network, we used the time-of-flight (TOF) imaging. Leveraging the contrast between fresh spins of blood and surrounding tissues, we employed high-resolution TOF with isotropic resolution of 0.38 mm to produce vivid images of arteries, as demonstrated in Figures 5. This approach enabled us to identify arteries such as the posterior cerebral artery (PCA) with diameters between 2-3 mm, anterior choroidal artery (AChA), diameter 0.7-2mm, and various branches of the PCA, diameter 1mm (Spallazzi et al., 2019), with notable limitations in detecting smaller arteries below 0.5 mm due to the resolution constraints.

Post-mortem studies by Erdem (Erdem et al., 1993) and further classifications by (Isolan et al., 2020), our investigation classified hippocampal arterial vasculature according to distinct groups. Our analysis, uses a single hemisphere in each of the 8 participants, unveiled patterns of arterial supply aligned with five out of the six groups delineated by Isolan et al. (2020). The PCA emerged as the primary source of hippocampal supply, often accompanied by contributions from AChA. Three out of our 8 participants were classified as group F which is the most common group found in this study.

Moreover, the importance of Susceptibility-Weighted Imaging (SWI) for visualizing the small veins encircling the hippocampus, a goal that has previously usually required the use contrast agents (Buch et al., 2020, Shen et al., 2020, Buch et al., 2022, Liu et al., 2018, Buch et al., 2021) or only been possible in cadaver studies (Wen et al., 1999). Figures 5.9 to 5.17 show the utility of 7T 3D GRE with a resolution of 0.38 x 0.37 x 0.74 mm for generating SWI and visualizing these intricate structures. While the need for high resolution impacted signal-to-noise ratio (SNR), a consistent pattern of veins was identified, particularly around the basal vein. In this work we used a single threshold across the image, but it is possible that an local thresholding might provide improvements.

Our findings correspond well to the superficial arteries and veins extracted from a cadaver hippocampus (Wen et al., 1999), as illustrated in Figure 5. The PCA and its associated branches were prominently delineated, while the AChA, basal vein, and subependymal intrahippocampus vein were also identified. This shows the potential, validity and utility of our preliminary investigation in portraying the hippocampal vasculature.

V. Conclusion

In essence, this preliminary study serves as a foundational stepping stone toward potential advancements in comprehending the complex interplay between hippocampal vasculature and degenerative pathologies, all propelled by the application of non-contrast imaging methods. By shedding light on the intricate vascular networks within the hippocampus, our findings not only open avenues for further explorations but also underscore the practicability of gleaning invaluable insights from these imaging modalities. Furthermore, our study paves the way for investigating variations into the diameters of arteries and veins among individuals with neurodegenerative diseases, potentially illuminating whether these changes could serve as pivotal triggers for such conditions.

References

- [1] Braak, H., & Braak, E. (1991). Acta H ' Pathologica Neuropathological Stageing Of Alzheimer-Related Changes. In Acta Neuropathol (Vol. 82).
- [2] Buch, S., Chen, Y., Jella, P., Ge, Y., & Haacke, E. M. (2022). Vascular Mapping Of The Human Hippocampus Using Ferumoxytol-Enhanced Mri: Intra-Hippocampal Vascular Density. *Neuroimage*, 250(January), 118957. <https://doi.org/10.1016/j.neuroimage.2022.118957>
- [3] Buch, S., Subramanian, K., Jella, P. K., Chen, Y., Wu, Z., Shah, K., Bernitsas, E., Ge, Y., & Haacke, E. M. (2021). Revealing Vascular Abnormalities And Measuring Small Vessel Density In Multiple Sclerosis Lesions Using Uspio. *Neuroimage: Clinical*, 29(November 2020), 102525. <https://doi.org/10.1016/j.nicl.2020.102525>
- [4] Buch, S., Wang, Y., Park, M. G., Jella, P. K., Hu, J., Chen, Y., Shah, K., Ge, Y., & Haacke, E. M. (2020). Subvoxel Vascular Imaging Of The Midbrain Using Uspio-Enhanced Mri. *Neuroimage*, 220(March), 117106. <https://doi.org/10.1016/j.neuroimage.2020.117106>
- [5] Erdem, A., Gazi, M., & Roth, P. (1993). Microsurgical Anatomy Of The Ethmoid. *Surgical And Radiologic Anatomy*, 15(1), 9–14. <https://doi.org/10.1007/Bf01629855>
- [6] Fulop, G. A., Ahire, C., Csipo, T., Tarantini, S., Kiss, T., Balasubramanian, P., Yabluchanskiy, A., Farkas, E., Toth, A., Nyúl-Tóth, Á., Toth, P., Csiszar, A., & Ungvari, Z. (2019). Cerebral Venous Congestion Promotes Blood-Brain Barrier Disruption And Neuroinflammation, Impairing Cognitive Function In Mice. *Geroscience*, 41(5), 575–589. <https://doi.org/10.1007/S11357-019-00110-1>
- [7] Haacke, E. M., Xu, Y., Cheng, Y. C. N., & Reichenbach, J. R. (2004). Susceptibility Weighted Imaging (Swi). *Magnetic Resonance In Medicine*, 52(3), 612–618. <https://doi.org/10.1002/mrm.20198>
- [8] Henri Duvernoy, Françoise Cattin, P.-Y. R. (2013). The Human Hippocampus. In *Vascularisation* (3rd Ed., Pp. 69–105). Springer Nature Switzerland.
- [9] Isolan, G. R., Stefani, M. A., Schneider, F. L., Claudino, H. A., Yu, Y. H., Choi, G. G., Telles, J. P. M., Rabelo, N. N., & Figueiredo, E. G. (2020). Hippocampal Vascularization: Proposal For A New Classification. *Surgical Neurology International*, 11(378), 1–6. https://doi.org/10.25259/Sni_708_2020
- [10] Jack, C. R., Wengenack, T. M., Reyes, D. A., Garwood, M., Curran, G. L., Borowski, B. J., Lin, J., Preboske, G. M., Holasek, S. S., Adriany, G., & Poduslo, J. F. (2005). Neurobiology Of Disease In Vivo Magnetic Resonance Microimaging Of Individual Amyloid Plaques In Alzheimer's Transgenic Mice. <https://doi.org/10.1523/Jneurosci.2588-05.2005>
- [11] Jenkinson, M., Bannister, P., Brady, M., & Smith, S. (2002). Improved Optimization For The Robust And Accurate Linear Registration And Motion Correction Of Brain Images. *Neuroimage*, 17(2), 825–841. <https://doi.org/10.1006/nimg.2002.1132>
- [12] Liu, S., Brisset, J. C., Hu, J., Haacke, E. M., & Ge, Y. (2018). Susceptibility Weighted Imaging And Quantitative Susceptibility Mapping Of The Cerebral Vasculature Using Ferumoxytol. *Journal Of Magnetic Resonance Imaging*, 47(3), 621–633. <https://doi.org/10.1002/jmri.25809>
- [13] Manjon, J. V., Romero, J. E., & Coupe, P. (2020). Deephips: A Novel Deep Learning Based Hippocampus Subfield Segmentation Method. February. <http://arxiv.org/abs/2001.11789>
- [14] Marinković, S., Milisavljević, M., & Puškaš, L. (1992). Microvascular Anatomy Of The Hippocampal Formation. *Surgical Neurology*, 37(5), 339–349. [https://doi.org/10.1016/0090-3019\(92\)90001-4](https://doi.org/10.1016/0090-3019(92)90001-4)
- [15] Prades, J. M., Veyret, C., & Martin, C. (1993). Microsurgical Anatomy Of The Ethmoid. *Surgical And Radiologic Anatomy*, 15(1), 9–14. <https://doi.org/10.1007/Bf01629855>
- [16] Shen, Y., Hu, J., Eteer, K., Chen, Y., Buch, S., Alhourani, H., Shah, K., Jiang, Q., Ge, Y., & Haacke, E. M. (2020). Detecting Sub-Voxel Microvasculature With Uspio-Enhanced Susceptibility-Weighted Mri At 7 T. *Magnetic Resonance Imaging*, 67(September 2019), 90–100. <https://doi.org/10.1016/j.mri.2019.12.010>
- [17] Spallazzi, M., Dobisch, L., Becke, A., Berron, D., Stucht, D., Oeltze-Jafra, S., Caffarra, P., Speck, O., & Düzel, E. (2019). Hippocampal Vascularization Patterns: A High-Resolution 7 Tesla Time-Of-Flight Magnetic Resonance Angiography Study. *Neuroimage: Clinical*, 21(May 2018). <https://doi.org/10.1016/j.nicl.2018.11.019>
- [18] Wen, H. T. M. , Rhoton, A. L. J. M. , De Oliveira, E. M. , Cardoso, A. C. C. M. , & Tedeschi, H. M. . (1999). Microsurgical

- Anatomy Of The Temporal Lobe: Part 1: Mesial Temporal Lobe Anatomy And Its Vascular Relationships As Applied To Amygdalohippocampectomy (P. 549). *Neurosurgery*.
- [19] Yushkevich, P. A., Pluta, J. B., Wang, H., Xie, L., Ding, S. L., Gertje, E. C., Mancuso, L., Kliot, D., Das, S. R., & Wolk, D. A. (2015). Automated Volumetry And Regional Thickness Analysis Of Hippocampal Subfields And Medial Temporal Cortical Structures In Mild Cognitive Impairment. *Human Brain Mapping*, 36(1), 258–287. <https://doi.org/10.1002/hbm.22627>
- [20] Zhang, X., Yin, X., Zhang, J., Li, A., Gong, H., Luo, Q., Zhang, H., Gao, Z., & Jiang, H. (2019). High-Resolution Mapping Of Brain Vasculature And Its Impairment In The Hippocampus Of Alzheimer's Disease Mice. *National Science Review*, 6(6), 1223–1238. <https://doi.org/10.1093/nsr/nwz124>